Magmatic History and Crustal Genesis of Western South America: Constraints from U-Pb ages and Hf Isotopes of Detrital Zircons in Modern Rivers

Martin Pepper, George Gehrels, Alex Pullen, Mauricio Ibanez-Mejia, Kevin M. Ward, and Paul Kapp

Supplemental Item 4: Continuous Wavelet Transform Analysis

In this supplemental item, we provide additional results from our continuous wavelet transform (CWT) analysis of the Northern, Central, and Southern Andean sections presented in the main text as well as a brief description of CWT analysis (Figs. S1-S4). Traditional Fourier analysis implicitly assumes any physical relationships are stationary in time. The wavelet method employed in our analysis has several advantages over traditional Fourier analysis and is particularly well-suited for analyzing geological and geophysical time-series that may exhibit periodic behavior which varies in time with localized intermittent periodicities (Torrence & Compo, 1998). For each individual time-series, we calculate the continuous (local) wavelet power spectrum. Because the wavelet is not everywhere localized in time, we define a cone of influence (COI), where edge effects are significant. We also define a ≥95% confidence interval using a first order autoregressive process (Allen & Smith, 1996) that models red noise (random walk noise) to identify statistically significant areas of signal generated wavelet power. The continuous (local) wavelet power spectrum results for each individual time-series analyzed show signal power at similar periods as the Lomb-Scargle periodograms (Fig. 7) with additional information about localized intermittent periodicities.

The CWT analyses described above provide statistically significant information about localized intermittent periodicities. To explore potential mechanistic explanations of the magmatic records from South America, we employ two approaches of analyzing pairs of CWTs generated from individual time-series; the cross wavelet transform (XWT) and the wavelet coherence (WTC). Here we briefly describe these two approaches and refer the interested reader to Grinsted et al. (2004) for a more detailed formal mathematical description. The XWT provides a statistically significant measure (≥95% confidence interval against red noise) of the common power between two CWTs as a function of period and time. Both the XWT and WTC have the additional property of returning the phase difference between signals with common

power/coherence, also as a function of period and time. This information is helpful in establishing a mechanistic connection as any cause and effect relationship would be phase locked, meaning the phase (time lag) would be constant for any period with statistically significant common power/coherence. The WTC extends the analysis of XWT to time-series with significant coherence even if the common power is low. The WTC is analogous to traditional correlation coefficients with the added property of quantifying correlation within localized intermittent periodicities.

Diagrams with the results of our analyses of magmatic history and convergence rate for NA, CA, and SA are provided on Figures A1-A3. These comparisons lead to the following conclusions:

1. All three transects show periodicities of magmatism and convergence rates that are similar to those shown on the periodograms of Figure 7. All three transects show a dominant periodicity of convergence rate of ~20 m.y. (Figs. S1d-S3d). Although harder to identify in this CWT analysis, the dominant periods of magmatism (Figs. S1c-S3c) are consistent with ~25, ~21, and ~34 m.y. (from the Northern, Central, and Southern Andean sections, respectively) obtained using the Lomb-Scargle least-squares spectral analysis (Fig. 7).

2. The cross-wavelet transforms (Figs. S1e-S3e) highlight periods where both time series have common power allowing for a first-order analysis of how well the two time-series in comparison are correlated. Although the convergence rate and age distribution times series have similar power of ~20 m.y. in the Northern and Central sections (Figs. S1e-S2e), and to a lesser extent in the Southern section (Fig. S3e), the time series are not phase locked (e.g. all black arrows pointing in the same direction for a specific period) where they have similar power (black closed contours). This indicates the relationship between the way the two time-series are behaving is changing with time and is not consistent with a simple causative relationship.

3. As we are comparing time-series with very different physical mechanisms, it is still possible that a correlation may exist, even where there is no common power shared between the signals. The wavelet coherence diagrams (Figs. S1f-S3f) are a more sophisticated way of analyzing two time-series as they can identify signals that are correlated while simultaneously lacking similar power. The results of our WTC (Figs. S1f-S3f) unambiguously show there is no such correlation consistent with a simple causative relationship between convergence rates and age distribution (see Figure S4f for an example of a strong correlation between two-time series).

We accordingly conclude that there is little evidence for genetic linkages between magmatic histories and convergences rates. Similar analyses that compare magmatic history with the age of the downgoing oceanic and the absolute motion of South America also reveal little correlation.

To further highlight the lack of a statistically significant correlation between the convergence rates and magmatic histories of the Andean margin, we show a CWT analysis (Fig. S4) for two time-series where a correlation is both visually observable and expected. Convergence rates along the Central and Northern sections are expected to have a strong correlation as the relative plate motions for the two-plate system (South American plate versus Pacific/Nazca Plates) should not change much between the Northern and Central sections of the margin. Visually, the convergence rates track each other (Figs. S4a-b) and show a similar power around a period of 20 m.y. (Figs. S4c-e) supporting the periodograms shown in Figure 7 of the main text. It is worth noting that a statistically significant correlation is observed for the two convergence rates (as expected) and that the correlation is in phase (black arrows pointing to the right) and phase locked (for a given period, all arrows point the same direction). This indicates the relationship between the way the two time-series are behaving is stationary with time and is consistent with a simple causative relationship.

All CWT analysis were generated in Matlab using the freely available software and methods developed in Grinsted et al. (2004) For a more detailed formal mathematical description and practical examples of the codes used, we refer the interested reader to the following reference: http://www.glaciology.net/wavelet-coherence.

References Cited

Allen, M.R. and Smith, L.A., 1996, Monte Carlo SSA: Detecting irregular oscillations in the presence of coloured noise: Journal of Climate, v. 9, p. 3373–3404.

Grinsted, A., Moore, J.C., and Jevrejeva S., 2004, Application of the cross wavelet transform and wavelet coherence to geophysical time series: Nonlinear Processes in Geophysics, v. 11, p. 561-566.

Torrence, C., Compo, G.P., 1998, A practical guide to wavelet analysis: Bulletin of the American Meteorological Society, v. 79, p. 61-78.

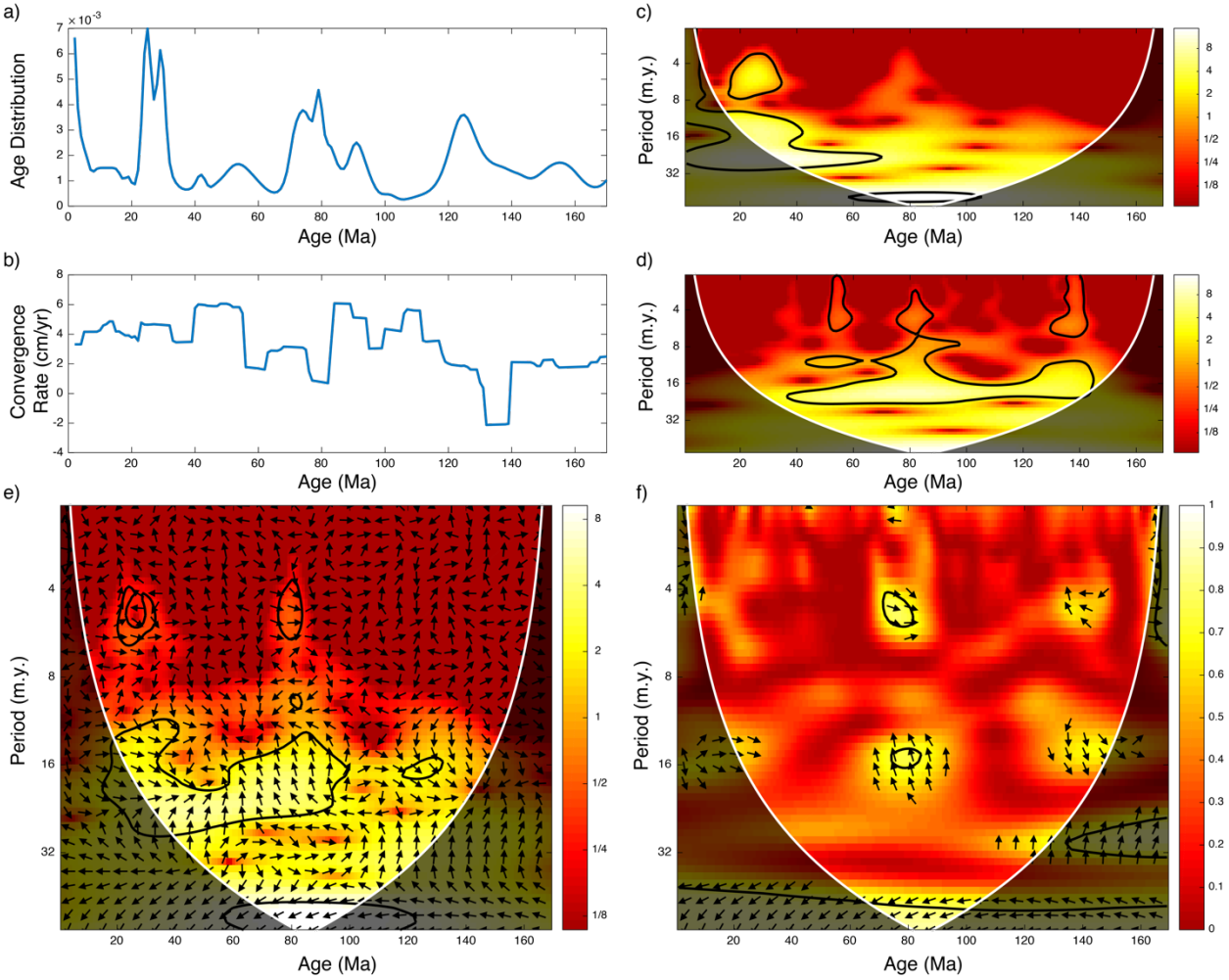

Figure S1. Results of our continuous wavelet transform (CWT) analysis for the Northern Andean (CA) section. Magmatic history (A) and convergence rate (B) time-series used in CWT analysis, (C and D) continuous wavelet power for the A and B time-series, (E) cross wavelet transform of the two time-series, and (F) wavelet coherence of the two time-series. The ≥95% confidence interval against red noise is shown as a thick black contour. The cone of influence (COI), where edge effects are significant, is shown as a masked white section. Phase differences are shown as black arrows where in-phase arrows point to the right and anti-phase (180° out-of-phase) arrows point to the left.

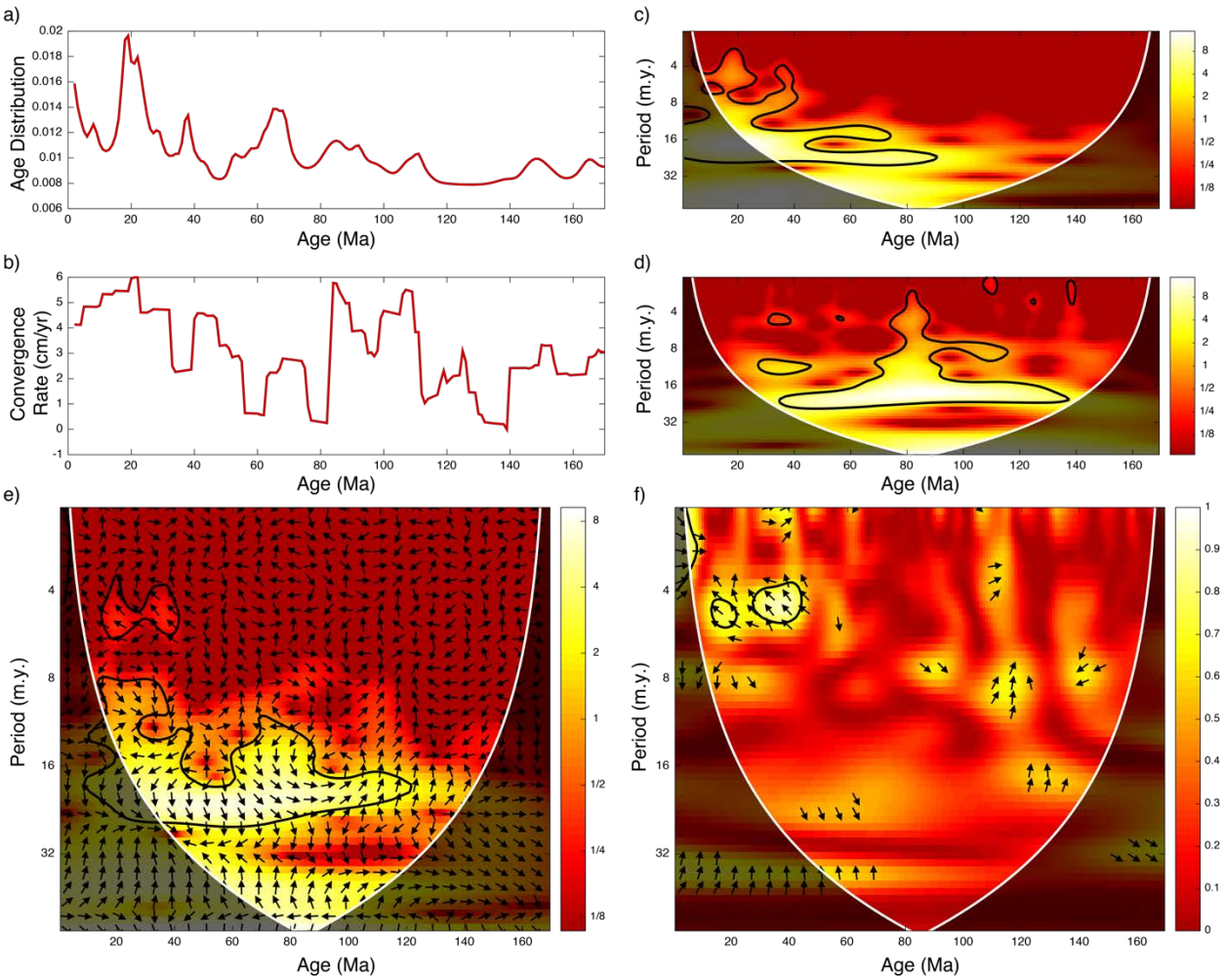

Figure S2. Results of our continuous wavelet transform (CWT) analysis for the Central Andean (CA) section (also shown in main text (Figure 15)). Magmatic history (A) and convergence rate (B) time-series used in CWT analysis, (C and D) continuous wavelet power for the A and B time-series, (E) cross wavelet transform of the two time-series, and (F) wavelet coherence of the two time-series. The ≥95% confidence interval against red noise is shown as a thick black contour. The cone of influence (COI), where edge effects are significant, is shown as a masked white section. Phase differences are shown as black arrows where in-phase arrows point to the right and anti-phase (180° out-of-phase) arrows point to the left.

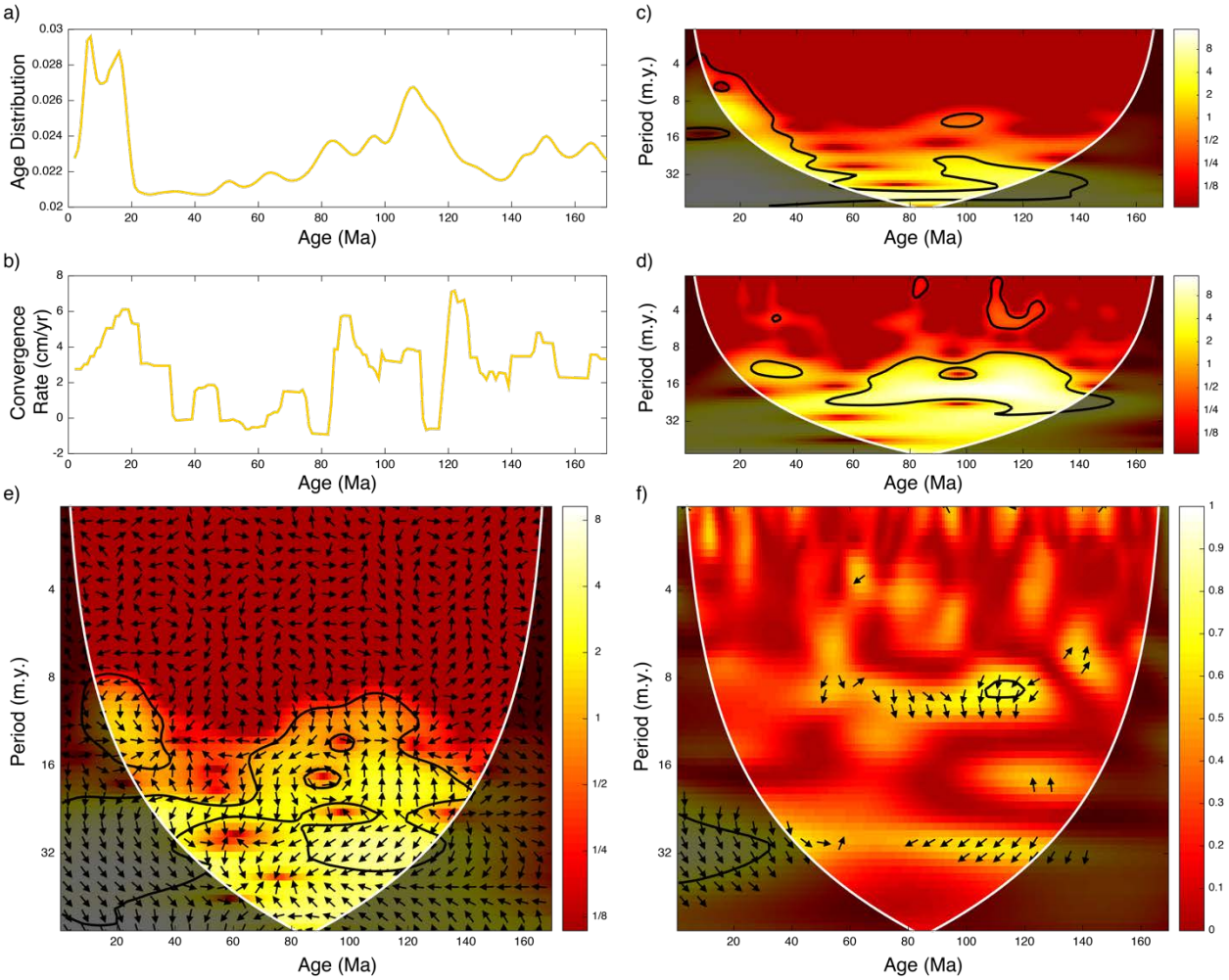

Figure S3. Results of our continuous wavelet transform (CWT) analysis for the Southern Andean (CA) section. Magmatic history (A) and convergence rate (B) time-series used in CWT analysis, (C and D) continuous wavelet power for the A and B time-series, (E) cross wavelet transform of the two time-series, and (F) wavelet coherence of the two time-series. The ≥95% confidence interval against red noise is shown as a thick black contour. The cone of influence (COI), where edge effects are significant, is shown as a masked white section. Phase differences are shown as black arrows where in-phase arrows point to the right and anti-phase (180° out-of-phase) arrows point to the left.

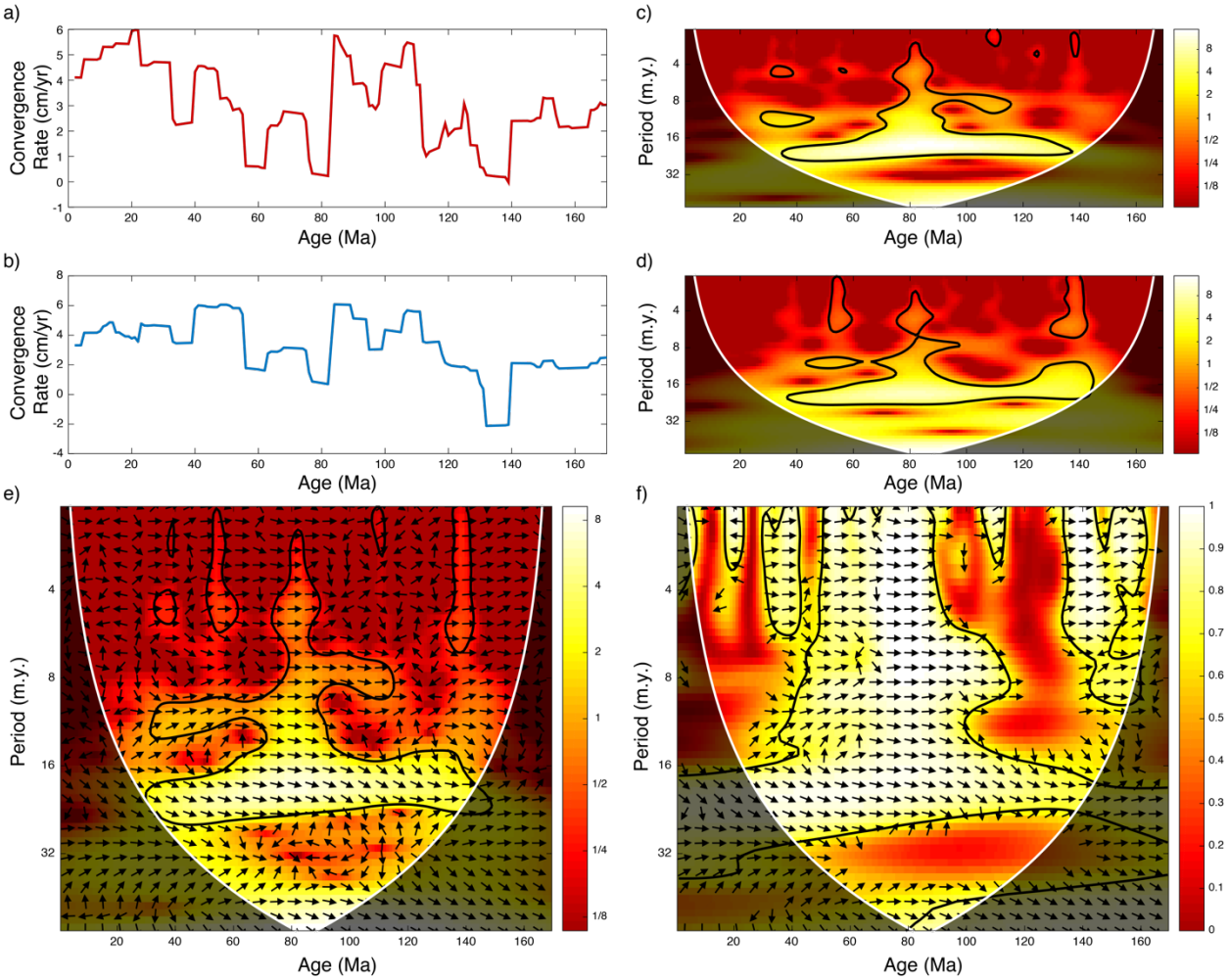

Figure S4. Results of our continuous wavelet transform (CWT) analysis for the convergence rates of the Central (CA) and Northern Andean (NA) sections. CA convergence rate (A) and NA convergence rate (B) time-series used in CWT analysis, (C and D) continuous wavelet power for the A and B time-series, (E) cross wavelet transform of the two time-series, and (F) wavelet coherence of the two time-series. The ≥95% confidence interval against red noise is shown as a thick black contour. The cone of influence (COI), where edge effects are significant, is shown as a masked white section. Phase differences are shown as black arrows where in-phase arrows point to the right and anti-phase (180° out-of-phase) arrows point to the left.